Hindawi
Journal of Nanomaterials
Volume 2017, Article ID 7492515, 9 pages
https://doi.org/10.1155/2017/7492515

Research Article

Structural and Antimicrobial Evaluation of Silver Doped Hydroxyapatite-Polydimethylsiloxane Thin Layers

S. L. Iconaru,[1] M. C. Chifiriuc,[2,3] and A. Groza[4]

[1]*National Institute of Materials Physics, P.O. Box MG 07, Bucharest, 077125 Magurele, Romania*
[2]*Microbiology Department, Faculty of Biology, University of Bucharest, 1-3 Portocalelor Lane, 77206 Bucharest, Romania*
[3]*Life, Environmental and Earth Sciences Division, Research Institute of the University of Bucharest (ICUB), 91-95 Splaiul Independentei, Bucharest, Romania*
[4]*National Institute for Laser, Plasma and Radiation Physics, 409 Atomistilor St., P.O. Box MG 36, 077125 Magurele, Romania*

Correspondence should be addressed to A. Groza; andreea@infim.ro

Received 5 April 2016; Revised 10 June 2016; Accepted 19 January 2017; Published 7 March 2017

Academic Editor: Simo-Pekka Hannula

An Ag:HAp ($x_{Ag} = 0.5$) powder was deposited by thermal evaporation technique as coating on a silicon substrate previously covered with a polydimethylsiloxane (PDMS) layer. The Ag:HAp-PDMS layers were characterized by Scanning Electron Microscopy (SEM), Energy Dispersive X-ray Spectroscopy (EDS), and Fourier Transform Infrared Spectroscopy (FT-IR). By infrared spectroscopy analysis, the phase composition of the Ag:HAp-PDMS layers was investigated. The antimicrobial activity of Ag:HAp-PDMS layers was tested against *Escherichia coli*, *Staphylococcus aureus,* and *Candida albicans* microbial strains. The microbial activity decreases significantly for the surveyed time intervals on Ag:HAp-PDMS layers.

1. Introduction

During the last decades the need for newly and improved materials with application in the medical field has increased due the constant and rapid progress of modern medicine [1, 2]. Each year new metallic implant systems are designed to be tested and accredited for clinical use. Therefore, the attention of researchers worldwide has been focused on developing novel materials which could serve as biocompatible coatings, combining nanotechnology and materials science [3–5]. In the present day, metal prostheses are successfully used in orthopedic surgeries and dentistry. For that purpose, various hybrid materials have been investigated in order to be used as biocompatible surface coatings for metallic implants. The most representative class of materials often applied to increase the biocompatibility of prostheses and implants is those based on calcium phosphate, in particular hydroxyapatite (HAp). Having the molecular formula $Ca_{10}(PO_4)_6(OH)_2$, HAp is known to be both biocompatible and bioactive and hydroxyapatite coatings are now used in various biomedical applications in orthopedic surgeries, dental surgeries, and craniomaxillofacial reconstructions [6, 7]. One of the major problems encountered in the case of implants are postoperatory infections. The apparition of infection could cause serious problems and if not treated properly could call for reopening the surgery which is both risky and uncomfortable for both the patients and the doctors.

Various bacteria such as *Escherichia coli (E. coli)* and *Staphylococcus aureus (S. aureus)* are a major concern to the patients' well-being. Also, a frequent cause of infection acquired in hospitals is contamination with fungi, especially with *Candida albicans (C. albicans)* [8–10]. This life-threatening fungus is considered in United States to be the fourth most frequently encountered cause of systemic infections acquired from hospitals [8–11]. It is responsible for deep tissue and mucosal infections being associated with biofilm growth [12]. Thus, the solutions for fighting against bacteria and fungi are imperatively necessary.

In order to avoid postoperatory infections, the use of biomedical devices with good antimicrobial properties is very important. The most studied element for its excellent

antimicrobial properties is silver. It has been extensively used as an antimicrobial agent in many medical devices such as wound dressings, cardiac prostheses, bone cements, catheters, and orthopedic fixation pins [13–15]. Although HAp is a bioactive material, an approach to improve the osseointegration, the mechanical properties, and the antimicrobial activity is to chemically modify HAp by doping it with low levels of beneficial elements. Various substitutions with elements such as Ag, Cu, Zn, or Si in the HAp lattice play an important role in its biological activity, influencing solubility, antimicrobial properties, surface chemistry, and particle morphology of this material. One of the proposed solutions for preventing the development of postoperatory infections was to embed silver ions (Ag^+) in the structure of HAp and then use the silver doped hydroxyapatite nanoparticles as coatings for the metallic implants.

Even though several different deposition techniques such as magnetron sputtering, pulsed laser deposition, electrohydrodynamic spray deposition, and biomimetic routes have been investigated in recent years in order to obtain thin coatings, there are still many examination to be made regarding the bioactivity, osteoconduction, and mechanical strength of the coatings. Recent studies showed that the use of polydimethylsiloxane (PDMS) as interfacial layers can substantially increase the adhesion, strength, and resistance of HAp coatings [16–20].

PDMS is an elastomer with proven biocompatibility properties frequently used for biological studies [21] being preferred as soft substrate for culturing different types of cells due to its nontoxicity and biodegradability [22]. It presents chemical and thermal stability (due to the strength of the Si-O bonds [23–26]), low surface energy, hydrophobicity (mainly due to the methyl groups present in its structure), and physiological inertness [23, 24]. It is used in various biomedical implants since the 1960s [25].

In our previous papers we showed that the use of PDMS as an interlayer between a HAp coating and a substrate may improve the delamination of HAp layers even when the substrate is rough [18, 20]. It was shown that the polymer acts as a matrix in which the HAp is incorporated. The hardness (H) of the composite layer increased while its Young's modulus (Y) decreased [19]. In the physicochemical analysis of these layers, respectively, the XRD measurements showed that the crystalline form of the HAp is maintained in the composite layer [18]. It is important to notice that these results were obtained using a Ag:HAp nanopowder treated thermally at 800°C [19].

On the basis of previous results, in this paper we report the generation and characterization of the silver doped hydroxyapatite with PDMS (Ag:HAp-PDMS) layers obtained by thermal evaporation technique starting from Ag:HAp nanopowders not previously thermally treated. As the absence of the thermal treatment of the Ag:HAp powder can influence the physicochemical properties of the Ag:HAp coatings, in this paper we investigate the morphological and structural properties of the deposited layers by Scanning Electron Microscopy, Energy Dispersive X-ray Spectroscopy (EDS), and Fourier Transform Infrared Spectroscopy (FT-IR). In comparison with our previous studies regarding the Ag:HAp and Ag:HAp-PDMS layers antimicrobial activity against *C. albicans* [19], the present work presents not only the antifungal activity against *C. Albicans* strain but also the antibacterial activity against *S. aureus* and *E. coli* strains of the Ag:HAp and Ag:HAp-PDMS layers.

2. Experimental

2.1. Deposition of PDMS Polymer Layer on Commercially Pure Si Disks. The experimental set-up described in [27] consists in a point to plane corona discharge electrode configuration. The deposition of PDMS polymer layers on commercially pure Si disks has been performed in agreement with Groza et al. [28].

2.2. Silver Doped Hydroxyapatite (Ag:HAp) Nanoparticles. In order to synthesize the silver doped hydroxyapatite (Ag:HAp), precursors of calcium nitrate [$Ca(NO_3)_2 \cdot 4H_2O$, Aldrich, USA], ammonium hydrogen phosphate ($(NH_4)_2HPO_4$ (Wako Pure Chemical Industries Ltd.)), and $AgNO_3$ (Alpha Aesare, Germany, 99.99% purity) were used.

The method of silver doped hydroxyapatite nanopowder generation was presented in detail in [29].

2.3. Deposition of Ag:HAp Nanoparticles on a Silicon Substrate Previously Coated with a PDMS Layer. The Ag:HAp ($x_{Ag} = 0.5$) powder has been deposited by thermal evaporation technique on a silicon substrate previously coated with a PDMS layer. The Ag:HAp nanoparticles are evaporated in vacuum. A HOCH VACUUM Dresden installation was used under environmental conditions. The pressure in the deposition chamber was in the range of $8 \cdot 10^{-5}$ torr. The time range for a deposition cycle was around 120 sec. The Ag:HAp powder evaporation temperature was 1100°C.

The evaporation time measured during deposition is situated in the range of 20 sec for a maximum current intensity of $I = 75$ A and in the range of 15 sec for an 80 A maximum current. Taking into account the deposition characteristics such as the total amount of HAp deposited (in mg) and the substrate-boat distance, the calculated evaporation velocities are $v_1 = 0.167$ mg/s or $v_1 \sim 8.3$ nm/s.

In the presence of the PDMS layer, which partially covers (on a circular surface with 10 mm in diameter) the Si substrate (with a diameter of 20 mm), the evaporated Ag:HAp nanoparticles diffuse into the polymer during their travel to the substrate. When the Ag:HAp particles stop into the polymer layer they transfer their energy to the polymer. Thus, the local temperature increases and, as the polymer is heated, the thermal condition of a new compound generation is assured.

2.4. Samples Characterization. The morphology of the material was studied using a Quanta Inspect F Scanning Electron Microscope (SEM) equipped also with an EDAX/2001 device.

Elemental compositional analysis was done using energy dispersive X-ray spectroscopy (EDS).

The IR spectra of the Ag:HAp-PDMS composite layers formed on silicon substrates have been obtained using an IR

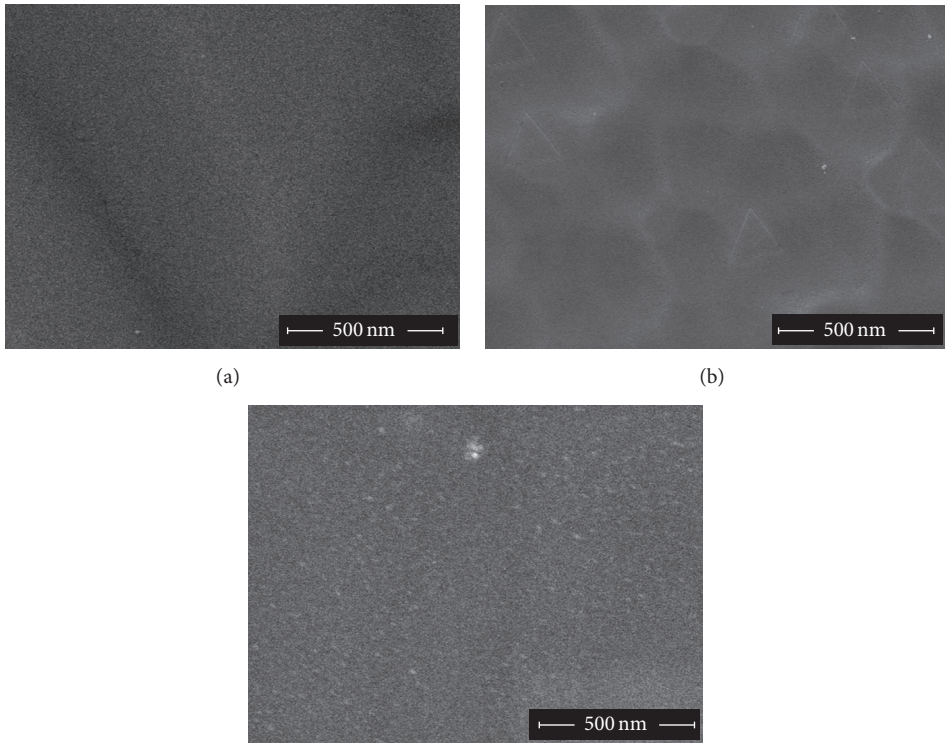

Figure 1: SEM images of Ag:HAp layer (a); PDMS layer (b); and Ag:HAp-PDMS composite (c) layer deposited on Si substrates.

Perkin Elmer SP 100 spectrometer equipped with a variable angle specular reflectance accessory. The FT-IR spectra of the Ag:HAp, PDMS and Ag:HAp-PDMS layers presented in this paper were registered at an incident angle of the light on the samples of 30°. In order to highlight the presence of PDMS and Ag:HAp specific IR bands into the IR spectrum of Ag:HAp-PDMS composite layer, in the 500–800 cm^{-1} and 800–1200 cm^{-1} spectral ranges was performed a peak fitting analysis applying the following procedure [30]: (i) baseline correction, (ii) second derivative calculation and self-deconvolution assessment in order to determine the number and positions of the bands, and (iii) curve fittings with fixed peak positions using Lorentzian functions.

2.5. Antimicrobial Assay. The antimicrobial assays of the *C. albicans, S. aureus, and E. coli* were performed using microtiter twofold serial dilutions method and were quantified after 24 and 48 hours, respectively, [31–35]. The microbial suspensions densities were measured spectrophotometrically at 492 nm and 620 nm [31–35].

3. Results and Discussions

The microstructure and the morphology of the thin films were investigated by Scanning Electron Microscopy. In Figure 1 is presented the microstructure of the obtained thin films ((a) Ag:HAp layer; (b) PDMS layer; and (c) Ag:HAp-PDMS composite layer) on Si substrates. It is obvious that the thin films are continuous and that the polymer layer acts as a matrix for the Ag:HAp nanoparticles. Also, it could be observed that the layers are homogeneous. The obtained results are in good agreement with the previous studies conducted by Iconaru et al. [36].

The EDS spectra of Ag:HAp coating in the presence, respectively, and the absence of the PDMS layer are presented in Figures 2(a) and 2(b). In both spectra can be identified the Ag, P, and Ca elements specific to Ag:HAp coatings. In Figure 2(b), the Si, O, and C peaks associated with the PDMS layer are also present. The presence of the PDMS polymer does not affect the structure of Ag:HAp coating.

The functional groups present in the prepared samples were revealed by FT-IR measurements performed in the absorbance mode. In Figure 3 is shown the spectrum recorded for the silver doped hydroxyapatite sample deposited on a Si substrate in the range 500–2000 cm^{-1}. The peaks observed in the regions 450–650 cm^{-1} and 950–1100 cm^{-1} prove that the studied sample has a well-crystallized apatitic phase. The peaks registered at 603 and 568 cm^{-1} are characteristic to the ν_4 mode of the PO_4^{3-} group. Moreover, previous studies [36–38] have shown that the separation of these two peaks proves the presence of a highly crystallized apatitic phase. Also, the peaks from 1037 and 1097 cm^{-1} are attributed to the ν_3 mode of the PO_4^{3-} functional group [39, 40]. The presence of CO_3^{2-} group is manifested by the peaks found in the region 1400–1600 cm^{-1} and at around 870 cm^{-1} [39].

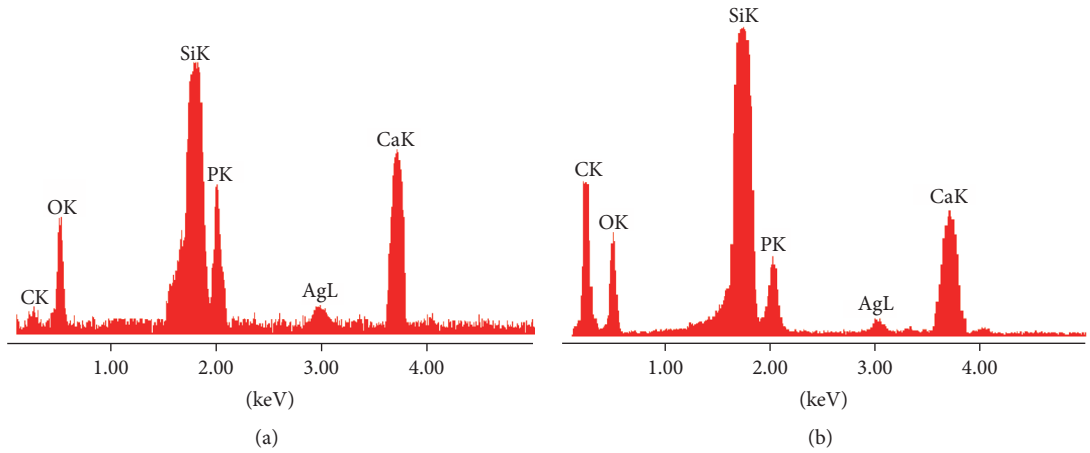

Figure 2: EDS spectra of (a) Ag:HAp and (b) Ag:HAp-PDMS layers.

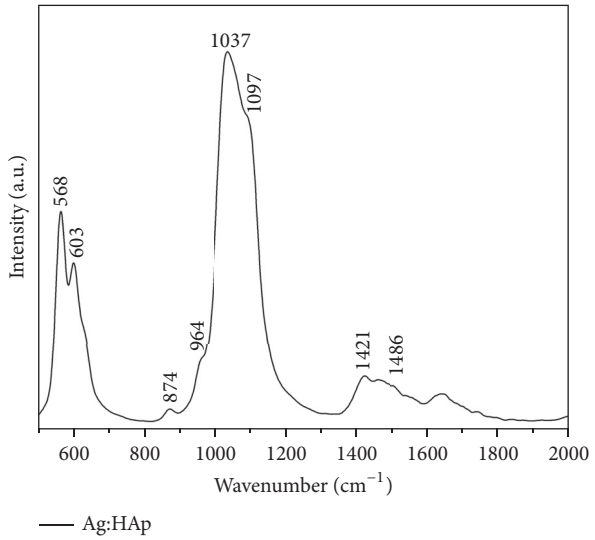

Figure 3: FT-IR spectrum of silver doped hydroxyapatite sample deposited on a Si substrate in the range 500–2000 cm^{-1}.

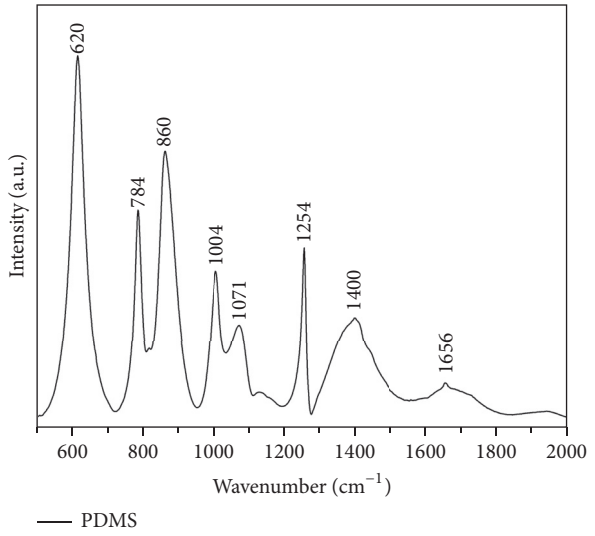

Figure 4: FT-IR spectrum of PDMS deposited on a Si plate.

The polymer has been deposited on a Si plate and its structure has been also studied by FT-IR spectroscopy (Figure 4). After analyzing the obtained spectrum, it has been observed the presence of different functional groups. Thus, the bands registered at 1254 and 1400 cm^{-1} are attributed to the symmetrical and asymmetrical deformation of the CH_3 bond from the Si-CH_3 group [41]. Furthermore, the presence of the Si-C stretching vibration from the same functional group is evidenced by the 784 cm^{-1} and 860 cm^{-1} absorption bands. The IR band observed at 620 cm^{-1} corresponds to the asymmetric stretching vibration of $Si(CH_3)_2$ group [42]. The presence of the Si-O-Si vibrations associated with the siloxane bonds is related to the bands from 1004 and 1071 cm^{-1} [42]. The large band at around 1650 cm^{-1} can be assigned to the OH groups.

The structure of the Ag:HAp-PDMS composite layer deposited on the Si substrate has also been evidenced by FT-IR measurements. In Figure 5 is shown the obtained spectrum where peaks attributed both to the PDMS polymer and to silver doped hydroxyapatite can be observed. The peaks found in the region 500–660 cm^{-1} are characteristic to the PO_4^{3-} group and the those observed in the region 1400–1600 cm^{-1} are associated with the ν_3 asymmetric stretching vibration of the carbonate functional group [39], both present in the Ag:HAp nanocomposite [36, 43]. On the other hand, the band found at 695 cm^{-1} indicates the presence of a crystalized SiO_2 based material [18, 44]. Also, the bands from around 800 cm^{-1} and those observed in the region 900–1200 cm^{-1} prove the presence of SiO_4^{4-} functional group in the studied sample [18, 44]. The peak observed at around 870 cm^{-1} is determined by an overlapping of two distinct

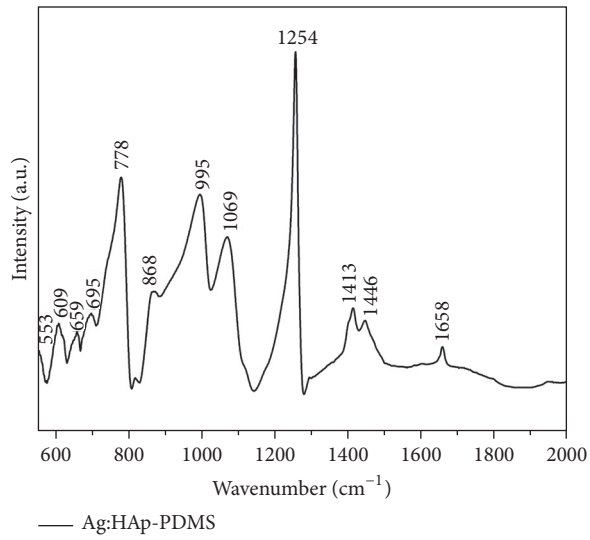

Figure 5: FT-IR spectrum of Ag:HAp-PDMS layer.

bands (the band from 862 cm^{-1} attributed to Si-O bonds [45] from the PDMS polymer and the band from 870 cm^{-1} associated with the carbonate functional group found in the Ag:HAp nanocomposite [36, 46]). The strong peak from 1254 cm^{-1} is characteristic to the CH_3 bond present in the structure of the polymer [42]. The large band at around 1650 cm^{-1} is assigned to the water lattice present in the samples.

A peak fitting analysis of the IR spectrum of the Ag:HAp-PDMS layer from Figure 5 has been performed in the range of 500–800 cm^{-1} and 800–1150 cm^{-1}, the results being presented in Figure 6. In this way, the contribution of each PDMS and HAp IR specific bands to the overall spectrum of the Ag:HAp-PDMS layer is better evidenced. In Figure 6(a), the IR bands from 568, 603 and 647 cm^{-1} correspond to the P-O vibrations into the PO_4^{3-} group. The deconvoluted band from 659 cm^{-1} was previously assigned to HAp [47] and the one from 695 cm^{-1} is specific to SiO_2 [44]. The overlapping of the bands from 740 cm^{-1} (Si-O/Si-CH_3 [48]), around 770 cm^{-1} (Si-O [44]) and 784 cm^{-1} (Si-C/Si-O-P [18]), could be an indication of the Si based structures incorporation into the Ag:HAp [49, 50]. The deconvoluted spectrum from Figure 6(b) also indicates the overlapping of the IR bands specific to HAp and PDMS. Thus the bands from 903, 964, and 1040 cm^{-1} correspond to P-O vibrations in PO_4^{3-} [18] while those from 1004, 1071, and 1120 cm^{-1} are specific to Si-O-Si, respectively, Si-O bonds [18].

Various factors such as certain bacterial strains of pneumococcus, meningococcus type B, "Haemophilus influenza" or bacterial proteins with enzymatic activity (e.g., protease, hyaluronidase, neuraminidase, elastase, and collagenase) can facilitate the invasion of microbial infections when there are defects in defence mechanisms or low resistance to microbial agents. Numerous microorganisms have mechanisms that impair antibody production by inducing suppressor cells. More than that, the adherence of microbial molecules to the surface plays a role in the development of microbial strains. The immediate immune response to bacterial infection is affected by a defect in the phagocytic system and can produce the development of severe pneumonias or recurrent abscesses. The binding of certain Gram-positive organisms (e.g., staphylococci) is favoured by host receptors such as cell surface proteins or cell surface sugar residues. Bacteria such as *Escherichia coli* possess distinctive adhesive organelles called fimbriae or pili that allow them to attach to almost all human cells including neutrophils and epithelial cells in the genitourinary tract, mouth, and intestine. On the other hand, *S. aureus* is a type of bacteria commonly found on hair, skin, noses, and throats of people and animals and it multiplies rapidly at room temperature. *S. aureus* can cause serious food poisoning. Moreover, it is one of the most common causes of infections in the hospitals and may cause diseases.

The fungal infections are divided into different groups depending on the type of fungus involved. *C. albicans* is a common fungus that often lives in mouth, stomach, skin, women's vaginas, or rectum. Usually, it does not cause any problems. However, *C. albicans* can displace through the blood stream and affect the throat, intestines, and heart valves. When there is some change in the body environment, this fungus can be a threat, becoming an infectious agent.

Firstly, the microbial activity of the silver doped hydroxyapatite-polydimethylsiloxane (Ag:HAp-PDMS) layers against *S. aureus 0364*, *E. coli ATCC 25922,* and *C. albicans 10231* was evaluated (Figures 7(a) and 7(b)).

We can see that the obtained Ag:HAp-PDMS layer on Si substrate proved to exhibit superior resistance to *S. aureus 0364*, *E. coli ATCC 25922,* and *C. albicans 10231* as compared to Si substrate or PDMS layers deposited on Si substrate (Si-PDMS). The antimicrobial activity gradually decreased when it was measured after 24 h and 48 h, respectively, as demonstrated by the lower absorbance values obtained after 48 h for Ag:HAp-PDMS layers (Figure 7(b)) compared to those obtained after 24 h (Figure 7(a)). On the Si-PDMS layer and Si substrate the antimicrobial activity was not observed and no significant differences were noticed neither after 24 h nor after 48 h.

Secondly, we have chosen to assess the antibiofilm activity of the Ag:HAp-PDMS layers on Si substrate, PDMS layers on Si substrate (Si-PDMS), and Si substrate (Si) against *S. aureus 0364*, *E. coli ATCC 25922,* and *C. albicans 10231* (Figures 8(a) and 8(b)).

It can be observed that the inhibition of the microbial biofilm development is gradually increasing from 24 h to 48 h. The Ag:HAp-PDMS layers on Si substrate proved to exhibit superior resistance to microbial colonization as compared with Si-PDMS layers and Si substrate (Si) against *S. aureus 0364*, *E. coli ATCC 25922,* and *C. albicans 10231.* Moreover, on the Si-PDMS and Si substrate, no important distinction was observed for the biofilms developed after 24 h and 48 h, respectively. The results of Ag:HAp-PDMS composite layers against *S. aureus 0364*, *E. coli ATCC 25922,* and *C. albicans 10231* showed great inhibition after 24 h and 48 h.

Recent studies performed by Ciobanu et al. [51] on silver doped hydroxyapatite nanoparticles have proven a good antimicrobial activity for all the studied concentrations

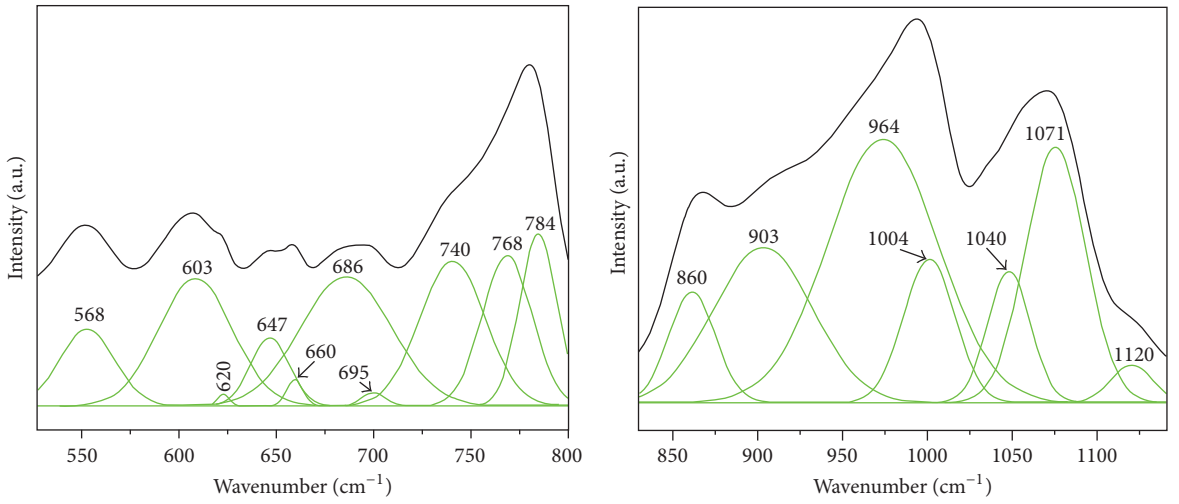

Figure 6: Deconvoluted IR spectra of Ag:HAp-PDMS layers in the spectral region of: (a) 450–800 cm^{-1}; (b) 800–1150 cm^{-1}.

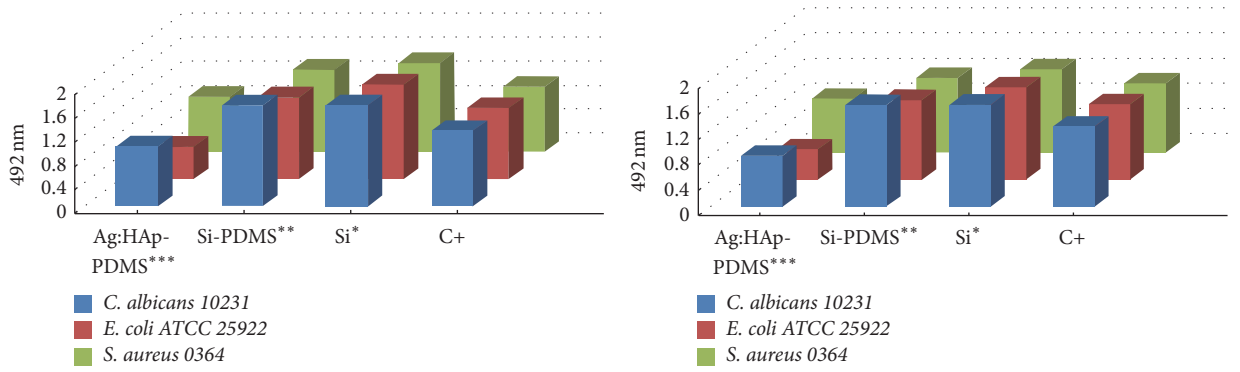

Figure 7: The graphic representation of the microbial activity of *S. aureus 0364*, *E. coli ATCC 25922*, and *C. Albicans 10231* on Ag:HAp-PDMS layers on Si substrate, PDMS layers on Si substrate (Si-PDMS), and Si substrate (Si) at 24 h (a) and 48 h (b). *silicon substrate, **silicon substrate previously coated with PDMS, and ***Ag:HAp nanoparticles on a silicon substrate previously coated with a PDMS layer.

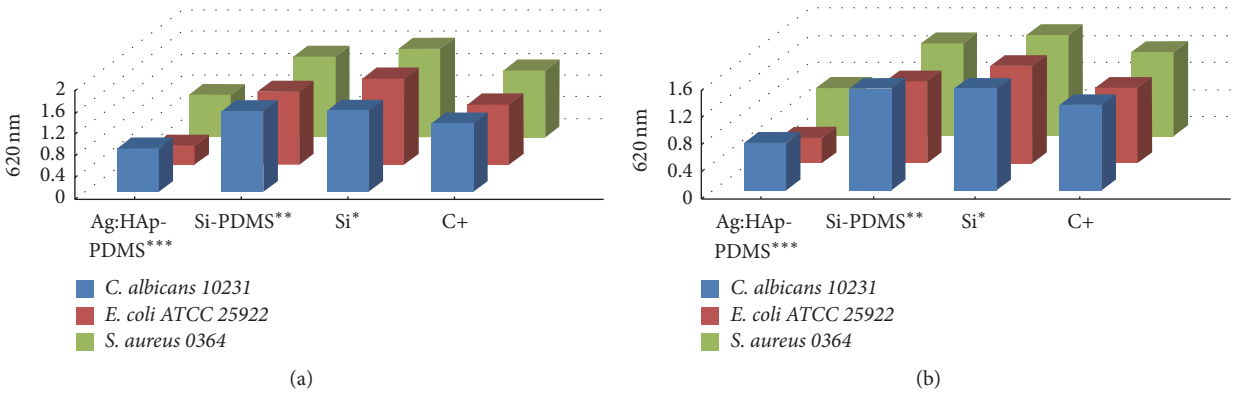

Figure 8: The inhibition of the microbial biofilm development at 24 h (a) and 48 h (b). *silicon substrate, **silicon substrate previously coated with PDMS, and ***Ag:HAp nanoparticles on a silicon substrate previously coated with a PDMS layer.

of silver in the samples. Moreover, recent studies on hydroxyapatite doped with samarium and europium have also demonstrated a good antimicrobial activity [39]. We could thus say that Ag:HAp-PDMS layers could be used for covering the surface of implantable medical devices. Future studies will be focused on creating a new substrate such as europium and samarium doped hydroxyapatite and PDMS layers that prevent the development of microbial strains.

4. Conclusions

In this paper, the results concerning the structural, morphological, and biological properties of Ag:HAp-PDMS composite layers are presented. The Ag:HAp-PDMS nanocomposite layers were deposited on commercially pure Si disks by thermal evaporation technique using an Ag:HAp nanopowder not thermally treated. The SEM studies proved that the prepared thin films are homogeneous and continuous, the PDMS polymer acting as a matrix for the Ag:HAp nanoparticles. The EDS and FT-IR spectral analysis of the investigated layers revealed the chemical elements and structure of the Ag:HAp-PDMS coating. The IR spectrum of the Ag:HAp-PDMS layer comprise bands characteristic to both Ag:HAp and PDMS and evidenced the Si-O-P interlink bonds formation.

Biological investigations were performed on various antimicrobial strains. To this end, some of the most commonly bacterial and fungal strains were selected. The microbial activities of *S. aureus 0364*, *E. coli ATCC 25922,* and *C. Albicans 10231* on Ag:HAp-PDMS composite layer were studied. It was demonstrated that the Ag:HAp-PDMS coating exhibited superior resistance to *S. aureus 0364*, *E. coli ATCC 25922,* and *C. albicans 10231* as compared to Si substrate or PDMS layers deposited Si substrate (Si-PDMS). On the other hand, the inhibition of the microbial biofilm development was assessed for the Ag:HAp-PDMS composite layer against the studied microbial strains. The results of this assay proved that the Ag:HAp-PDMS composite layers showed great inhibition after 24 and 48 h against *S. aureus 0364*, *E. coli ATCC 25922,* and *C. albicans 10231*.

Competing Interests

The authors declare that they have no competing interests.

Acknowledgments

The studies reported in this paper have been funded by the Projects PN II 259/2014 and PN-III-P2-2.1-PTE-2016-0177. The authors wish to thank Mrs. Dr. Daniela Predoi for the proof reading of the manuscript, valuable discussions, and suggestions. The authors are thankful to Dr. R. Ghita and Dr. C. S. Ciobanu for SEM and FT-IR measurements and for helping in the fabrication of the Ag:HAp nanopowders. Furthermore, the authors thank Cristina Liana Popa for her contribution to the synthesis of Ag:HAp nanopowders.

References

[1] A. F. Von Recum, C. E. Shannon, C. E. Cannon, K. J. Long, T. G. Van Kooten, and J. Meyle, "Surface roughness, porosity, and texture as modifiers of cellular adhesion," *Tissue Engineering*, vol. 2, no. 4, pp. 241–253, 1996.

[2] M. Long and H. J. Rack, "Titanium alloys in total joint replacement—a materials science perspective," *Biomaterials*, vol. 19, no. 18, pp. 1621–1639, 1998.

[3] D. Predoi, "Physico-chemical studies of sucrose thin films," *Digest Journal of Nanomaterials and Biostructures*, vol. 5, pp. 373–377, 2010.

[4] M. Putkonen, T. Sajavaara, P. Rahkila et al., "Atomic layer deposition and characterization of biocompatible hydroxyapatite thin films," *Thin Solid Films*, vol. 517, no. 20, pp. 5819–5824, 2009.

[5] D. Predoi, "A study on iron oxide nanoparticles coated with dextrin obtained by coprecipitation," *Digest Journal of Nanomaterials and Biostructures*, vol. 2, no. 1, pp. 169–173, 2007.

[6] N. A. Trujillo, R. A. Oldinski, H. Ma, J. D. Bryers, J. D. Williams, and K. C. Popat, "Antibacterial effects of silver-doped hydroxyapatite thin films sputter deposited on titanium," *Materials Science and Engineering C*, vol. 32, no. 8, pp. 2135–2144, 2012.

[7] K. McLeod, S. Kumar, N. K. Dutta, R. St. C. Smart, N. H. Voelcker, and G. I. Anderson, "X-ray photoelectron spectroscopy study of the growth kinetics of biomimetically grown hydroxyapatite thin-film coatings," *Applied Surface Science*, vol. 256, no. 23, pp. 7178–7185, 2010.

[8] F. L. Mayer, D. Wilson, and B. Hube, "Candida albicans pathogenicity mechanisms," *Virulence*, vol. 4, no. 2, pp. 119–128, 2013.

[9] G. D. Brown, D. W. Denning, and S. M. Levitz, "Tackling human fungal infections," *Science*, vol. 336, no. 6082, p. 647, 2012.

[10] M. A. Pfaller and D. J. Diekema, "Epidemiology of invasive candidiasis: a persistent public health problem," *Clinical Microbiology Reviews*, vol. 20, no. 1, pp. 133–163, 2007.

[11] D. Predoi, C. L. Popa, and M. V. Predoi, "Ultrasound studies on magnetic fluids based on maghemite nanoparticles," *Polymer Engineering and Science*, 2017.

[12] L. P. Samaranayake, J. McCourtie, and T. W. MacFarlane, "Factors affecting the *in-vitro* adherence of *Candida albicans* to acrylic surfaces," *Archives of Oral Biology*, vol. 25, no. 8-9, pp. 611–615, 1980.

[13] E. S. Thian, J. Huang, Z. H. Barber, S. M. Best, and W. Bonfield, "Surface modification of magnetron-sputtered hydroxyapatite thin films via silicon substitution for orthopaedic and dental applications," *Surface and Coatings Technology*, vol. 205, no. 11, pp. 3472–3477, 2011.

[14] S. Mudenda, K. L. Streib, D. Adams, J. W. Mayer, R. Nemutudi, and T. L. Alford, "Effect of substrate patterning on hydroxyapatite sol-gel thin film growth," *Thin Solid Films*, vol. 519, no. 16, pp. 5603–5608, 2011.

[15] A. Mo, J. Liao, W. Xu, S. Xian, Y. Li, and S. Bai, "Preparation and antibacterial effect of silver–hydroxyapatite/titania nanocomposite thin film on titanium," *Applied Surface Science*, vol. 255, no. 2, pp. 435–438, 2008.

[16] J. V. Rau, M. Fosca, I. Cacciotti, S. Laureti, A. Bianco, and R. Teghil, "Nanostructured Si-substituted hydroxyapatite coatings for biomedical applications," *Thin Solid Films*, vol. 543, pp. 167–170, 2013.

[17] H. Li, S. Liu, J. Zhao, D. Li, and Y. Yuan, "Thermal degradation behaviors of polydimethylsiloxane-graft-poly(methyl methacrylate)," *Thermochimica Acta*, vol. 573, pp. 32–38, 2013.

[18] C. L. Popa, A. Groza, P. Chapon et al., "Physicochemical analysis of the polydimethylsiloxane interlayer influence on a hydroxyapatite doped with silver coating," *Journal of Nanomaterials*, vol. 2015, Article ID 250617, 10 pages, 2015.

[19] C. S. Ciobanu, A. Groza, S. L. Iconaru et al., "Antimicrobial activity evaluation on silver doped hydroxyapatite/polydimethylsiloxane composite layer," *BioMed Research International*, vol. 2015, Article ID 926513, 13 pages, 2015.

[20] A. Groza, C. S. Ciobanu, C. L. Popa et al., "Structural properties and antifungal activity against *Candida albicans* biofilm of different composite layers based on Ag/Zn doped hydroxyapatite-polydimethylsiloxanes," *Polymers*, vol. 8, no. 4, article 131, 2016.

[21] D. Fuard, T. Tzvetkova-Chevolleau, S. Decossas, P. Tracqui, and P. Schiavone, "Optimization of poly-di-methyl-siloxane (PDMS) substrates for studying cellular adhesion and motility," *Microelectronic Engineering*, vol. 85, no. 5-6, pp. 1289–1293, 2008.

[22] L. Ceseracciu, J. A. Heredia-Guerrero, S. Dante, A. Athanassiou, and I. S. Bayer, "Robust and biodegradable elastomers based on corn starch and polydimethylsiloxane (PDMS)," *ACS Applied Materials and Interfaces*, vol. 7, no. 6, pp. 3742–3753, 2015.

[23] Q. Chen, S. Liang, and G. A. Thouas, "Elastomeric biomaterials for tissue engineering," *Progress in Polymer Science*, vol. 38, no. 3-4, pp. 584–671, 2013.

[24] M. Andriot, S. H. Chao, A. R. Colas et al., "Silicones in industrial applications," in *Silicon-Based Inorganic Polymers*, R. De Jaeger and M. Gleria, Eds., pp. 61–161, Nova Science Publishers, New York, NY, USA, 2009.

[25] A. Mata, A. J. Fleischman, and S. Roy, "Characterization of polydimethylsiloxane (PDMS) properties for biomedical micro/nanosystems," *Biomedical Microdevices*, vol. 7, no. 4, pp. 281–293, 2005.

[26] Y. Zhao and X. Zhang, "Mechanical properties evolution of polydimethylsiloxane during crosslinking process," in *Proceedings of the Mechanics of Biological and Bio-Inspired Materials, Materials Research Society Symposium Proceedings (MRS '06)*, vol. DD06-07, Boston, Mass, USA, 2006.

[27] A. Groza, "Review of the processes identified during the polymerization of organic and organosilicon liquid films in atmospheric pressure air corona discharges," *Romanian Reports in Physics*, vol. 64, pp. 1227–1242, 2012.

[28] A. Groza, A. Surmeian, C. Diplasu et al., "Physico-chemical processes occurring during polymerization of liquid polydimethylsiloxane films on metal substrates under atmospheric pressure air corona discharges," *Surface and Coatings Technology*, vol. 212, pp. 145–151, 2012.

[29] C. Ciobanu, F. Massuyeau, L. Constantin, and D. Predoi, "Structural and physical properties of antibacterial Ag-doped nano-hydroxyapatite synthesized at 100∘C," *Nanoscale Research Letters*, vol. 6, no. 1, p. 613, 2011.

[30] J. Kolmas, A. Jaklewicz, A. Zima et al., "Incorporation of carbonate and magnesium ions into synthetic hydroxyapatite: the effect on physicochemical properties," *Journal of Molecular Structure*, vol. 987, no. 1-3, pp. 40–50, 2011.

[31] C. Saviuc, A. M. Grumezescu, C. M. Chifiriuc et al., "Hybrid nanosystem for stabilizing essential oils in biomedical applications," *Digest Journal of Nanomaterials and Biostructures*, vol. 6, no. 4, pp. 1657–1666, 2011.

[32] C. Saviuc, A. M. Grumezescu, A. Holban et al., "Phenotypical studies of raw and nanosystem embedded Eugenia carryophyllata buds essential oil antibacterial activity on Pseudomonas aeruginosa and Staphylococcus aureus strains," *Biointerface Research in Applied Chemistry*, vol. 1, pp. 111–118, 2011.

[33] C. Saviuc, I. Marinas, A. M. Grumezescu et al., "Phytochemical composition of the fennel fruits essential oil and its influence on prokariotic cells growth and pathogenic features," *Biointerface Research in Applied Chemistry*, vol. 2, pp. 300–305, 2012.

[34] R. M. Cornell and U. Schertmann, *Iron Oxides in the Laboratory: Preparation and Characterisation*, VCH, Weinheim, Germany, 1991.

[35] K. V. P. M. Shafi, A. Gedanken, R. Prozorov, and J. Balogh, "Sonochemical preparation and size-dependent properties of nanostructured $CoFe_2O_4$ particles," *Chemistry of Materials*, vol. 10, no. 11, pp. 3445–3450, 1998.

[36] S. L. Iconaru, P. Chapon, P. Le Coustumer, and D. Predoi, "Antimicrobial activity of thin solid films of silver doped hydroxyapatite prepared by sol-gel method," *The Scientific World Journal*, vol. 2014, Article ID 165351, 8 pages, 2014.

[37] J. D. Termine and A. S. Posner, "Infrared analysis of rat bone: age dependency of amorphous and crystalline mineral fractions," *Science*, vol. 153, no. 3743, pp. 1523–1525, 1966.

[38] R. Z. LeGeros, "Calcium phosphates in oral biology and medicine," *Monographs in Oral Science*, vol. 15, pp. 1–3, 1991.

[39] C. S. Ciobanu, C. L. Popa, and D. Predoi, "Sm:HAp nanopowders present antibacterial activity against *Enterococcus faecalis*," *Journal of Nanomaterials*, vol. 2014, Article ID 780686, 9 pages, 2014.

[40] X. Bai, K. More, C. M. Rouleau, and A. Rabiei, "Functionally graded hydroxyapatite coatings doped with antibacterial components," *Acta Biomaterialia*, vol. 6, no. 6, pp. 2264–2273, 2010.

[41] A. Groza, A. Surmeian, M. Ganciu, and I. I. Popescu, "Infrared spectral investigation of the linseed oil polymerization in a corona discharge in air at atmospheric pressure," *Europhysics Letters*, vol. 68, no. 5, 2004.

[42] G. Socrates, *Infrared Characteristic Group Frequencies*, John Wiley & Sons Ltd, Chichester, UK, 2nd edition, 1994.

[43] C. S. Ciobanu, S. L. Iconaru, P. Le Coustumer, and D. Predoi, "Vibrational investigations of silver-doped hydroxyapatite with antibacterial properties," *Journal of Spectroscopy*, vol. 1, no. 1, Article ID 471061, 2013.

[44] B. J. Saikia, G. Parthasarathy, and N. C. Sarmah, "Fourier transform infrared spectroscopic estimation of crystallinity in SiO_2 based rocks," *Bulletin of Materials Science*, vol. 31, no. 5, pp. 775–779, 2008.

[45] A. Hilonga, J.-K. Kim, P. B. Sarawade, and H. T. Kim, "Influence of annealing conditions on the properties of reinforced silver-embedded silica matrix from the cheap silica source," *Applied Surface Science*, vol. 256, no. 9, pp. 2849–2855, 2010.

[46] S. Hayakawa, T. Kanaya, K. Tsuru et al., "Heterogeneous structure and in vitro degradation behavior of wet-chemically derived nanocrystalline silicon-containing hydroxyapatite particles," *Acta Biomaterialia*, vol. 9, no. 1, pp. 4856–4867, 2013.

[47] R. Narayan, M. Singh, and J. McKittrick, *Advances in Bioceramics and Biotechnologies: Ceramic Transactions*, vol. 218, The The American Ceramic Society, Wiley, 2010.

[48] A. Groza and A. Surmeian, "Characterization of the oxides present in a polydimethylsiloxane layer obtained by polymerisation of its liquid precursor in corona discharge," *Journal of Nanomaterials*, vol. 2015, Article ID 204296, 8 pages, 2015.

[49] A. Balamurugan, A. H. S. Rebelo, A. F. Lemos, J. H. G. Rocha, J. M. G. Ventura, and J. M. F. Ferreira, "Suitability evaluation of sol-gel derived Si-substituted hydroxyapatite for dental and maxillofacial applications through in vitro osteoblasts response," *Dental Materials*, vol. 24, no. 10, pp. 1374–1380, 2008.

[50] N. Hijón, M. Victoria Cabañas, J. Peña, and M. Vallet-Regí, "Dip coated silicon-substituted hydroxyapatite films," *Acta Biomaterialia*, vol. 2, no. 5, pp. 567–574, 2006.

[51] C. S. Ciobanu, S. L. Iconaru, M. C. Chifiriuc, A. Costescu, P. Le Coustumer, and D. Predoi, "Synthesis and antimicrobial activity of silver-doped hydroxyapatite nanoparticles," *BioMed Research International*, vol. 2013, Article ID 916218, 10 pages, 2013.